

Magnetism of the antiferromagnetic spin- $\frac{1}{2}$ tetramer compound CuInVO_5

Masashi Hase,^{1,*} Masashige Matsumoto,² Akira Matsuo,³ and Koichi Kindo³

¹*National Institute for Materials Science, Tsukuba, Ibaraki 305-0047, Japan*

²*Department of Physics, Shizuoka University, Shizuoka 422-8529, Japan*

³*The Institute for Solid State Physics, The University of Tokyo, Kashiwa, Chiba 277-8581, Japan*

(Received 16 June 2016; revised manuscript received 26 October 2016; published 14 November 2016)

We measured the temperature dependence of the magnetic susceptibility and specific heat and the magnetic-field dependence of the magnetization of CuInVO_5 . An antiferromagnetically ordered state appears below $T_N = 2.7$ K. We observed a $\frac{1}{2}$ quantum magnetization plateau above 30 T at 1.3 K. We consider that the probable spin model for CuInVO_5 is an interacting spin- $\frac{1}{2}$ tetramer model. We evaluated values of the intratetramer interactions as $J_1 = 240 \pm 20$ K (antiferromagnetic) and $J_2 = -142 \pm 10$ K (ferromagnetic). The ground state of the isolated spin tetramer with the J_1 and J_2 values is spin singlet. The shrinkage of ordered magnetic moments by quantum fluctuation can be expected. Detectable low-energy longitudinal-mode magnetic excitations may exist in CuInVO_5 .

DOI: [10.1103/PhysRevB.94.174421](https://doi.org/10.1103/PhysRevB.94.174421)

I. INTRODUCTION

The interacting antiferromagnetic (AF) spin-dimer compounds TiCuCl_3 [1–5] and KCuCl_3 [6,7] show a pressure-induced or magnetic-field-induced magnetic quantum phase transition. Experimental observations [8–11] and the theoretical background [12,13] of massive longitudinal-mode magnetic excitations in the ordered state were reported for these compounds. The longitudinal mode and massless transverse modes (Nambu-Goldstone modes) [14] are related to fluctuations in the amplitude and phase of the order parameter, respectively. The longitudinal mode is the analog of the Higgs particle [15–17].

According to the results of theoretical investigations, the longitudinal mode can exist in interacting AF spin cluster systems that are realized in $\text{Cu}_2\text{Fe}_2\text{Ge}_4\text{O}_{13}$ and $\text{Cu}_2\text{CdB}_2\text{O}_6$ [18]. The spin systems in $\text{Cu}_2\text{Fe}_2\text{Ge}_4\text{O}_{13}$ [18] and $\text{Cu}_2\text{CdB}_2\text{O}_6$ [19–21] can be regarded as interacting AF spin tetramers (Fe-Cu-Cu-Fe and Cu-Cu-Cu-Cu tetramers, respectively). The shrinkage of ordered magnetic moments by quantum fluctuation is important for the appearance of the longitudinal mode. The ground state (GS) can be a spin-singlet state in isolated AF spin clusters. Therefore, some interacting spin cluster systems are advantageous for the longitudinal mode. An antiferromagnetically ordered state appears in $\text{Cu}_2\text{Fe}_2\text{Ge}_4\text{O}_{13}$ [22] and $\text{Cu}_2\text{CdB}_2\text{O}_6$ [19] in zero magnetic field under atmospheric pressure. The magnetic excitations in $\text{Cu}_2\text{Fe}_2\text{Ge}_4\text{O}_{13}$ have been investigated by inelastic neutron-scattering (INS) experiments on single crystals [22–25]. The longitudinal mode was not confirmed because of the small INS intensities due to the large excitation energies (> 15 meV) and because of the overlap of the transverse modes. The magnetic excitations in $\text{Cu}_2^{114}\text{Cd}^{11}\text{B}_2\text{O}_6$ were studied by INS experiments on its powder [21]. Although the results suggest the existence of the longitudinal mode, there was no conclusive evidence because powder was used. A single crystal suitable for the measurements of physical properties has not been reported.

We require further spin cluster compounds that have an antiferromagnetically ordered state and low-energy longitudinal-mode magnetic excitations. We focus on spin- $\frac{1}{2}$ tetramers because of the following magnetism. The Hamiltonian of a spin tetramer is expressed as

$$\mathcal{H} = J_1 S_2 \cdot S_3 + J_2 (S_1 \cdot S_2 + S_3 \cdot S_4). \quad (1)$$

When $J_1 > 0$ or $J_2 > 0$, the GS is the spin-singlet state. Therefore, the shrinkage of ordered moments can be expected in an ordered state generated by the introduction of intertetramer interactions. The ordered state is possible under the condition that the value of Δ is comparable to or less than that of an effective intercluster interaction [18]. Here Δ is the energy difference (spin gap) between the singlet GS and first-excited triplet states. The effective intercluster interaction is given by the sum of the products of the absolute value of each intercluster interaction ($|J_{\text{int},i}|$) and the corresponding number of interactions per spin (z_i) as $J_{\text{eff}} = \sum_i z_i |J_{\text{int},i}|$. The effective intercluster interaction is usually much smaller than the dominant intratetramer interactions. Therefore, Δ should be much smaller than the dominant intratetramer interactions for the appearance of the ordered state.

Figure 1 shows the eigenenergies of the excited states measured from the GS in an isolated spin- $\frac{1}{2}$ tetramer [26]. As shown in Fig. 1(a) for $J_1 > 0$, Δ/J_1 can be sufficiently small when J_2 has negative or small positive values. Even under a small J_{eff} , an ordered state is expected in a spin-tetramer compound for $J_1 > 0$ and $J_2 < 0$. The small Δ/J_1 is in contrast to $\Delta/J = 1$ in the AF spin- $\frac{1}{2}$ dimer given by $J S_1 \cdot S_2$. As shown in Fig. 1(a), the GS and first-excited states are well separated from the other excited states (ESs). This means that the low-energy physics can be described by an effective spin-dimer (singlet-triplet) system [18]. There are compounds that have spin- $\frac{1}{2}$ tetramers expressed as Eq. (1) and an ordered state. Examples are $\text{Cu}_2\text{CdB}_2\text{O}_6$ with $J_1 = 317 \pm 12$, $J_2 = -162 \pm 16$, and $T_N = 9.8$ K [19–21] and SeCuO_3 with $J_1 = 225$, $J_2 = 160$, and $T_N = 8$ K [27].

We can expect spin- $\frac{1}{2}$ tetramers in CuInVO_5 from its crystal structure [28]. The Cu^{2+} ions ($3d^9$) have localized spin- $\frac{1}{2}$. The positions of the Cu ions and the O ions connected

*HASE.Masashi@nims.go.jp

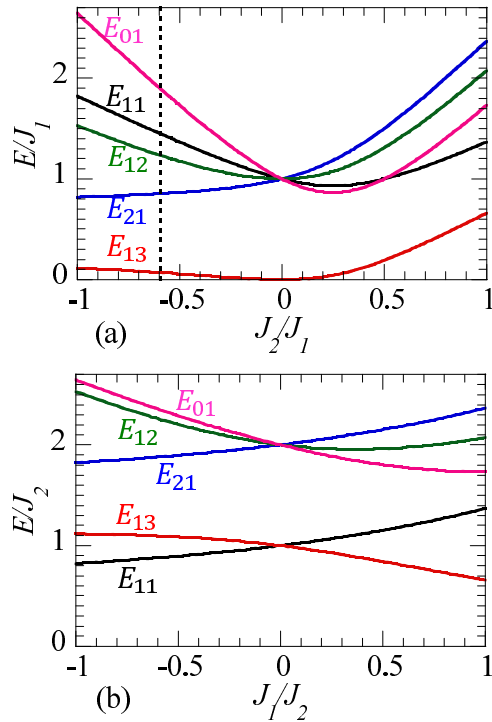


FIG. 1. Eigenenergies of excited states measured from the ground state in an isolated spin- $\frac{1}{2}$ tetramer expressed by Eq. (1). There are two $S^T = 0$ states ($|01\rangle$ and $|02\rangle$), three $S^T = 1$ states ($|11\rangle$, $|12\rangle$, and $|13\rangle$), and one $S^T = 2$ state ($|21\rangle$). S^T is the value of the sum of the spin operators in the tetramer. The eigenstates $|ij\rangle$ of the isolated tetramer are explicitly given in [26]. In the isolated tetramer, the ground state is the spin-singlet $|02\rangle$ state. (a) $J_1 > 0$. The vertical dashed line indicates the J_2/J_1 value of CuInVO_5 evaluated in the present work. (b) $J_2 > 0$.

to the Cu ions are shown schematically in Fig. 2(a). Two crystallographic Cu sites (Cu1 and Cu2) exist. Red and blue bars indicate the shortest and second-shortest Cu-Cu distances, respectively. The distances at room temperature are 3.117 and 3.173 Å, respectively. The closest Cu1-Cu1 pair is bridged by two identical Cu1-O-Cu1 paths the angle of which is 89.75°. The closest Cu1-Cu2 pair is bridged by two different Cu1-O-Cu2 paths with angles of 107.61 and 88.19°. The other Cu-Cu distances are 4.705 Å or greater. If dominant exchange interactions exist in the Cu1-Cu1 and Cu1-Cu2 pairs, spin tetramers given by Eq. (1) are formed. Figure 2(b) shows the arrangement of the spin tetramers. Two types of tetramers (I and II) exist, although they are equivalent to each other as a spin system. In this paper, we report the magnetism of CuInVO_5 . An AF long-range order appears below $T_N = 2.7$ K. We show that the spin system consists of spin tetramers with $J_1 > 0$ and $J_2 < 0$.

II. EXPERIMENTAL AND CALCULATION METHODS

Crystalline CuInVO_5 powder was synthesized by a solid-state reaction. Starting materials are CuO , In_2O_3 , and V_2O_5 powder. Their purity is 99.99%. A stoichiometric mixture of powder was sintered at 1023 K in air for 100 h with intermediate grindings. We measured an x-ray powder-diffraction

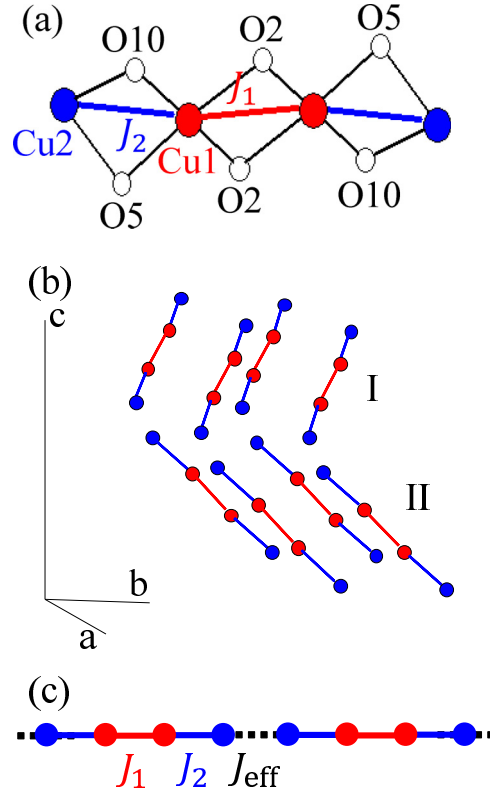


FIG. 2. (a) Schematic drawing of positions of Cu^{2+} and O^{2-} ions connected to Cu^{2+} ions in CuInVO_5 [28]. Red, blue, and white circles indicate Cu1, Cu2, and O sites, respectively. Red and blue bars represent the shortest and second-shortest Cu-Cu distances, respectively. Thin black bars represent Cu-O. We define J_1 and J_2 as the exchange interaction parameters for the Cu1-Cu1 and Cu1-Cu2 pairs, respectively. The J_1 and J_2 interactions form a spin- $\frac{1}{2}$ tetramer. (b) Schematic drawing of spin tetramers in CuInVO_5 . Two types of tetramers (I and II) exist, although they are equivalent to each other as a spin system. (c) Interacting spin tetramer model used to calculate magnetization using a mean-field theory based on the tetramer unit (tetramer mean-field theory).

pattern at room temperature using an x-ray diffractometer (RINT-TTR III, Rigaku). The wavelength is 1.540 and 1.544 Å ($\text{Cu } K\alpha_1$ and $K\alpha_2$ lines, respectively). X rays of $\text{Cu } K\beta$ are excluded. We adopted a flat sample scattering geometry. We performed Rietveld refinements based on the space group $P2_1/c$ (No. 14) as in the literature [28] using the FULLPROF SUITE program package [29] with its internal tables for scattering lengths. All observed reflections can be indexed on the basis of the published structure data of CuInVO_5 . We confirmed that our sample was a nearly single phase of CuInVO_5 . The lattice constants are $a = 8.776(1)$, $b = 6.158(1)$, $c = 15.268(1)$ Å, and $\beta = 106.48(1)^\circ$. These are almost the same as the values reported in the literature [28] [$a = 8.793(2)$, $b = 6.1542(6)$, $c = 15.262(2)$ Å, and $\beta = 106.69(2)^\circ$]. The atomic positions in our results are close to those in the literature. We measured the specific heat using a physical property measurement system (Quantum Design). We measured the magnetization in magnetic fields of up to 5 T using a superconducting quantum interference

device magnetometer magnetic property measurement system (Quantum Design). High-field magnetization measurements were conducted using an induction method with a multilayer pulsed field magnet installed at the Institute for Solid State Physics, the University of Tokyo.

We obtained the eigenenergies and eigenstates of isolated spin- $\frac{1}{2}$ tetramers using an exact diagonalization method [26]. We calculated the temperature T dependence of the magnetic susceptibility and the specific heat and the magnetic-field H dependence of the magnetization $M(H)$ using the eigenenergies and eigenstates. We calculated $M(H)$ for the model shown in Fig. 2(c) using a mean-field theory based on the tetramer unit (tetramer mean-field theory). Finite magnetic moments were initially assumed on the Cu sites in the tetramer. The mean-field Hamiltonian was then expressed by a 16×16 matrix form under consideration of the external magnetic field and the molecular field from the nearest-neighbor sites. The eigenstates of the mean-field Hamiltonian were used to calculate the expectation value of the ordered moments on the Cu sites. We continued this procedure until the values of the magnetic moments converged. We finally obtained a self-consistently determined solution for $M(H)$.

III. RESULTS AND DISCUSSION

The red circles in Figs. 3 and 4 show the T dependence of the specific heat $C(T)$ of CuInVO_5 in zero magnetic field and the magnetic susceptibility $\chi(T)$ in a magnetic field of $H = 0.01$ T, respectively. We can observe a peak in $C(T)$ at 2.7 K and a clear decrease in $\chi(T)$ below this temperature, indicating the occurrence of an AF long-range order. A broad maximum can be seen around 8 K in $C(T)$ and around 11 K in $\chi(T)$, indicating that the origin of the broad maximum in

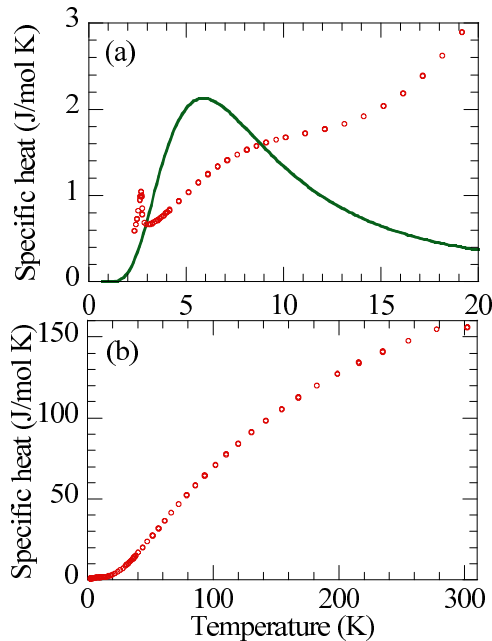


FIG. 3. Temperature T dependence of the specific heat $C(T)$ of CuInVO_5 in zero magnetic field. A green line indicates $C(T)$ calculated for an isolated spin- $\frac{1}{2}$ tetramer. The J_1 and J_2 values are listed in Table I.

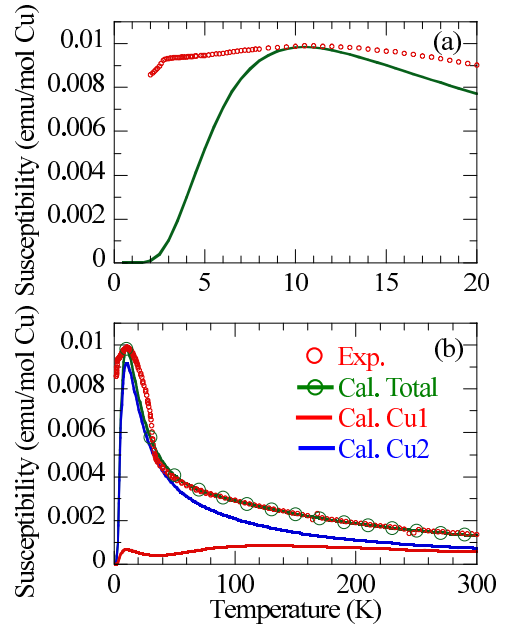


FIG. 4. Temperature T dependence of the magnetic susceptibility $\chi(T)$ of CuInVO_5 (circles) in a magnetic field of $H = 0.01$ T. Green, red, and blue lines indicate $\chi(T)$ calculated for the total, Cu1, and Cu2 spins, respectively, in an isolated spin- $\frac{1}{2}$ tetramer. The J_1 and J_2 values are listed in Table I.

$C(T)$ is magnetic. As T is increased, $\chi(T)$ decreases rapidly up to $T = 40$ K then decreases slowly at higher temperatures. Other phase transitions were not observed in $C(T)$ and $\chi(T)$ below 300 K.

The thick red lines in Figs. 5(a) and 5(b) show the H dependence of the magnetization $M(H)$ of CuInVO_5 measured at 1.3 and 30 K, respectively. We can observe a $\frac{1}{2}$ quantum magnetization plateau above 30 T at 1.3 K. The g value was evaluated to be 2.09 ± 0.02 from the magnetization of the plateau. The magnetization plateau is smeared at 30 K.

We compare $\chi(T)$, $C(T)$, and $M(H)$ for CuInVO_5 with those calculated for isolated spin tetramers. We calculated $\chi(T)$ for various sets of exchange parameters. The set in which $J_1 = 240$ and $J_2 = -142$ K is the best. The green line in Fig. 4(b) indicates $\chi(T)$ calculated for an isolated spin tetramer with $J_1 = 240$ and $J_2 = -142$ K. The J_1 and J_2 values are listed in Table I. The agreement between the experimental and calculated $\chi(T)$ is nearly perfect above 30 K, whereas a discrepancy is seen below 30 K. The green line in Fig. 3(a) indicates $C(T)$ calculated for the isolated spin tetramer with the same J_1 and J_2 values. The positions of the broad maximum in the experimental and calculated $C(T)$ are close to each other. However, the specific heat around the broad maximum is larger in the calculated result. Note that the experimental $C(T)$ contains not only the magnetic specific heat but also the lattice specific heat [30]. We calculated $C(T)$ for isolated spin tetramers with several sets of exchange parameters. The temperature of the maximum depends on the J_1 and J_2 values, whereas the height of the maximum is independent of the values. Similar results were obtained in other spin systems such as the AF uniform spin- $\frac{1}{2}$ chain [31]. Therefore, we did not estimate the J_1 and J_2 values in the specific-heat data.

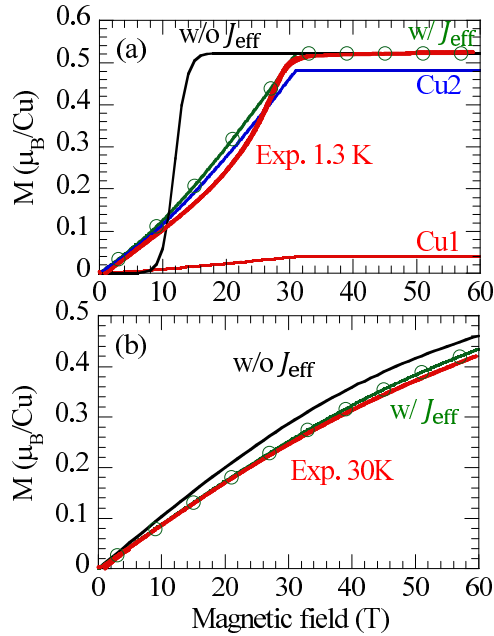


FIG. 5. Magnetic-field dependence of the magnetization of CuInVO_5 (thick red lines). Green, red, and blue lines indicate the magnetization calculated for the total, Cu1, and Cu2 spins, respectively, in the interacting spin- $\frac{1}{2}$ tetramer model in Fig. 2(c). Black lines indicate the magnetization calculated for an isolated spin- $\frac{1}{2}$ tetramer. The values of the exchange interactions are listed in Table I. (a) Magnetization at 1.3 K. (b) Magnetization at 30 K.

The black lines in Fig. 5 indicate $M(H)$ calculated for an isolated spin tetramer with the same J_1 and J_2 values. The calculated $M(H)$ is similar to the experimental $M(H)$ at 30 K, whereas the isolated spin tetramer model fails to reproduce the experimental $M(H)$ at 1.3 K. We could not find a set of exchange parameters that reproduced the experimental $M(H)$ at 1.3 K on the basis of an isolated tetramer.

The agreement between the experimental and calculated results in the susceptibility above 30 K indicates that the spin system in CuInVO_5 consists of spin tetramers with $J_1 = 240$ and $J_2 = -142$ K. To stabilize the ordered state, intertetramer interactions must exist in CuInVO_5 . Intertetramer interactions have a greater effect on the magnetization at lower T . Therefore, the discrepancy between the experimental results and those calculated for the isolated spin tetramer appears at low T . The magnetic structure of CuInVO_5 has not yet been reported. It is difficult to determine which intertetramer interactions are effective. Therefore, we assumed the simple model shown in Fig. 2(c) and calculated $M(H)$ using the tetramer mean-field

TABLE I. Values of exchange interaction parameters and g value. We used the central values for the calculations of the magnetic susceptibility in Fig. 4, the magnetization in Fig. 5, and the eigenenergies in Fig. 6.

| J_1 (K) | J_2 (K) | J_{eff} (K) | g |
|--------------|---------------|----------------------|-----------------|
| 240 ± 20 | -142 ± 10 | 30 ± 4 | 2.09 ± 0.02 |

theory. Since multiple intertetramer interactions are expected in CuInVO_5 , J_{eff} is the effective interaction between tetramers. As described below, the magnetic moment on Cu1 sites is small in the spin tetramer with $J_1 = 240$ and $J_2 = -142$ K. Therefore, we assumed intertetramer interactions between Cu2 spins. The green lines in Fig. 5 indicate $M(H)$ calculated for the interacting spin tetramer with $J_1 = 240$, $J_2 = -142$, and $J_{\text{eff}} = 30$ K. The experimental and calculated magnetizations are in agreement with each other at both 1.3 and 30 K.

We were not able to explain the experimental magnetic susceptibility below 30 K using the simple model shown in Fig. 2(c) and the tetramer mean-field theory because of the following reason. We evaluated $T_N = 8.7$ K for the simple model with the exchange interaction values in Table I using the tetramer mean-field theory. Mean-field theories become less valid for calculation of susceptibility when the temperature approaches T_N owing to strong fluctuations. A Monte Carlo simulation is one of the applicable theories near the transition temperature. It requires a set of realistic intertetramer interactions. As described, we do not know them. Therefore, we focus on the magnetization curve at low temperatures, where the ordered moment becomes substantial and the fluctuations are suppressed. The mean-field approximation becomes reliable. Therefore, we can reproduce $M(H)$ at 1.3 K with the effective intertetramer interaction $J_{\text{eff}} = 30$ K. We consider that our present model is idealized and not fully appropriate to explain the magnetism of CuInVO_5 . As a future study, we have to determine an interacting spin- $\frac{1}{2}$ tetramer model that can explain quantitatively the experimental susceptibility and magnetizations. We will mention this point later.

Figure 6 shows the eigenenergies of the excited states measured from the GS ($|02\rangle$ state) in the isolated spin tetramer with $J_1 = 240$ and $J_2 = -142$ K. The first excited states are the spin-triplet $|13\rangle$ states located at $\Delta = 17$ K. The condition for the appearance of the ordered state ($\Delta \leq J_{\text{eff}}$) is satisfied. The second excited states are the spin-quintet $|21\rangle$ states located at 205 K. The large energy difference between the first and second ESs generates the $\frac{1}{2}$ quantum magnetization plateau in Fig. 5(a).

We roughly estimated the errors of the J_1 , J_2 , and J_{eff} values and listed them in Table I. A discrepancy between the experimental and calculated $\chi(T)$ appears around 80 K when J_1 deviates from 240 K. The experimental and calculated $\chi(T)$ are not in agreement with each other when $J_1 = 220$ or 260 K. A discrepancy between the experimental and calculated $\chi(T)$

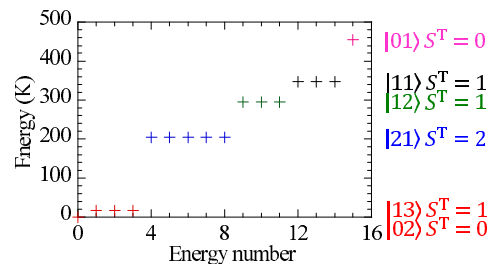


FIG. 6. Eigenenergies of the excited states measured from the ground state ($|02\rangle$ state) in the isolated spin- $\frac{1}{2}$ tetramer expressed by Eq. (1). The J_1 and J_2 values are listed in Table I.

appears around 11 K when J_2 deviates from -142 K. The peak heights of the experimental and calculated $\chi(T)$ are not in agreement with each other when $J_2 = -132$ or -152 K. The magnetic field at which the $\frac{1}{2}$ magnetization plateau appears increases with increasing J_{eff} . We roughly estimated the error of J_{eff} to be ± 4 K.

The results calculated for spins on the Cu1 and Cu2 sites are shown in Figs. 4(b) and 5(a). We used the isolated and interacting spin tetramers in the calculations of $\chi(T)$ and $M(H)$, respectively. Cu2 spins show much larger magnetization than Cu1 spins at low T . The maximum $\chi(T)$ around 11 K and the rapid decrease up to $T = 40$ K mainly originate from the Cu2 spins. As T is increased further, the susceptibility of Cu1 spins increases up to $T = 130$ K, whereas that of Cu2 spins decreases. Therefore, the total susceptibility shows weak T dependence between 50 and 100 K. The most dominant interaction is the J_1 interaction. The spin state of Cu1 spins is similar to the singlet state in AF dimers [32–34]. Therefore, the magnetization of Cu1 spins is small at low T . The two Cu2 spins in a tetramer are weakly and antiferromagnetically coupled to each other through a Cu1-Cu1 dimer in the same tetramer. Thus, the magnetization of Cu2 spins is large. The susceptibility and magnetization of CuInVO₅ resemble those of Cu₃(P₂O₆OH)₂, which has spin- $\frac{1}{2}$ trimerized chains expressed as the sequence -Cu(1)-Cu(2)-Cu(2)- [35,36]. The AF exchange interaction is largest between two neighboring Cu(2) spins (111 K). The magnetization of Cu(2) spins is small at low T . In each chain, two Cu(1) spins are weakly coupled to each other through an intermediate Cu(2)-Cu(2) AF dimer. The magnetization of Cu(1) spins is large.

In CuInVO₅, the low-energy triplet excitation is expected to have a finite gap above T_N as in Cu₂CdB₂O₆ [21]. When the temperature is decreased, the gap closes at T_N and the triplet excitation splits into a longitudinal mode and twofold degenerate transverse modes at $T < T_N$. Slightly below T_N , the ordered moment is small and the longitudinal mode is expected to be in the low-energy region (on the order of 1 meV). Thus, the ordered phase in CuInVO₅ corresponds to the pressure-induced ordered phase in TiCuCl₃ [1,2,9,10,12] and KCuCl₃ [6,11]. CuInVO₅ may be useful for studying the longitudinal mode under the atmospheric pressure.

The magnetic structure is necessary to calculate susceptibility and magnetic excitations. In future, we will determine the magnetic structure of CuInVO₅ by neutron powder-diffraction experiments. ¹¹⁵In atoms (natural abundance 95.7%) strongly absorb neutrons [the thermal absorption cross section is 202(2) barn for 0.0253 eV]. A thin sample with a large area is necessary for neutron-diffraction experiments to decrease effects of neutron absorptions. Powder is filled between two coaxial cylinders with different diameters (a double-wall container) to obtain a thin sample. It is expected to be possible to obtain diffraction patterns to determine the magnetic structure.

We will confirm the signs of J_1 and J_2 from the magnetic structure. The value of $|J_2/J_1|$ is the same as that of M_1/M_2 [20,22]. Here, M_1 and M_2 are magnitudes of ordered magnetic moments on Cu1 and Cu2 sites, respectively. After determination of the $|J_2/J_1|$ value, we will evaluate again J_1 and J_2 values from the experimental susceptibility at high temperatures. We will consider which intertetramer interactions are effective to stabilize the magnetic structure. We will calculate the magnetic susceptibility of more realistic models using quantum Monte Carlo techniques. We will confirm that the spin model for CuInVO₅ is an interacting spin- $\frac{1}{2}$ tetramer model. It is difficult to observe magnetic excitations by INS experiments because of the strong neutron absorption by ¹¹⁵In atoms. We intend to form single crystals of CuInVO₅ and perform Raman scattering experiments on them. We expect to observe one-magnon Raman scattering indicating longitudinal-mode magnetic excitations as in TiCuCl₃ [8] and KCuCl₃ [11].

IV. CONCLUSION

We measured the temperature dependence of the magnetic susceptibility and specific heat and the magnetic-field dependence of the magnetization of CuInVO₅. An antiferromagnetically ordered state appears below $T_N = 2.7$ K. We observed a $\frac{1}{2}$ quantum magnetization plateau above 30 T at 1.3 K. An isolated antiferromagnetic spin- $\frac{1}{2}$ tetramer model with $J_1 = 240$ and $J_2 = -142$ K can closely reproduce the magnetic susceptibility above 30 K. We were able to explain the magnetization curves using the interacting spin tetramer model with the effective intertetramer interaction $J_{\text{eff}} = 30$ K. We consider that the probable spin model for CuInVO₅ is an interacting spin- $\frac{1}{2}$ tetramer model. The value of the spin gap (singlet-triplet gap) is 17 K (1.5 meV) in the isolated spin tetramer. Detectable low-energy (on the order of 1 meV) longitudinal-mode magnetic excitations may exist in CuInVO₅.

ACKNOWLEDGMENTS

This work was financially supported by Japan Society for the Promotion of Science (JSPS) KAKENHI (Grants No. 23540396 and No. 15K05150) and by grants from National Institute for Materials Science. M.M. was supported by JSPS KAKENHI (Grant No. 26400332). The high-field magnetization experiments were conducted under the Visiting Researcher's Program of the Institute for Solid State Physics, the University of Tokyo. We are grateful to S. Matsumoto for sample syntheses and x-ray-diffraction measurements.

[1] H. Tanaka, K. Goto, M. Fujisawa, T. Ono, and Y. Uwatoko, Magnetic ordering under high pressure in the quantum spin system TiCuCl₃, *Physica B* **329–333**, 697 (2003).

[2] A. Oosawa, K. Kakurai, T. Osakabe, M. Nakamura, M. Takeda, and H. Tanaka, Pressure-induced successive magnetic phase transitions in the spin gap system TiCuCl₃, *J. Phys. Soc. Jpn.* **73**, 1446 (2004).

- [3] A. Oosawa, M. Ishii, and H. Tanaka, Field-induced three-dimensional magnetic ordering in the spin-gap system TiCuCl_3 , *J. Phys.: Condens. Matter* **11**, 265 (1999).
- [4] T. Nikuni, M. Oshikawa, A. Oosawa, and H. Tanaka, Bose-Einstein Condensation of Dilute Magnons in TiCuCl_3 , *Phys. Rev. Lett.* **84**, 5868 (2000).
- [5] H. Tanaka, A. Oosawa, T. Kato, H. Uekusa, Y. Ohashi, K. Kakurai, and A. Hoser, Observation of field-induced transverse Néel ordering in the spin gap system TiCuCl_3 , *J. Phys. Soc. Jpn.* **70**, 939 (2001).
- [6] K. Goto, M. Fujisawa, H. Tanaka, Y. Uwatoko, A. Oosawa, T. Osakabe, and K. Kakurai, Pressure-induced magnetic quantum phase transition in gapped spin system KCuCl_3 , *J. Phys. Soc. Jpn.* **75**, 064703 (2006).
- [7] A. Oosawa, T. Takamasu, K. Tatani, H. Abe, N. Tsujii, O. Suzuki, H. Tanaka, G. Kido, and K. Kindo, Field-induced magnetic ordering in the quantum spin system KCuCl_3 , *Phys. Rev. B* **66**, 104405 (2002).
- [8] H. Kuroe, K. Kusakabe, A. Oosawa, T. Sekine, F. Yamada, H. Tanaka, and M. Matsumoto, Magnetic field-induced one-magnon Raman scattering in the magnon Bose-Einstein condensation phase of TiCuCl_3 , *Phys. Rev. B* **77**, 134420 (2008).
- [9] Ch. Rüegg, B. Normand, M. Matsumoto, A. Furrer, D. F. McMorrow, K. W. Krämer, H.-U. Güdel, S. N. Gvasaliya, H. Mutka, and M. Boehm, Quantum Magnets under Pressure: Controlling Elementary Excitations in TiCuCl_3 , *Phys. Rev. Lett.* **100**, 205701 (2008).
- [10] P. Merchant, B. Normand, K. W. Krämer, M. Boehm, D. F. McMorrow, and Ch. Rüegg, Quantum and classical criticality in a dimerized quantum antiferromagnet, *Nat. Phys.* **10**, 373 (2014).
- [11] H. Kuroe, N. Takami, N. Niwa, T. Sekine, M. Matsumoto, F. Yamada, H. Tanaka, and K. Takemura, Longitudinal magnetic excitation in KCuCl_3 studied by Raman scattering under hydrostatic pressures, *J. Phys.: Conf. Ser.* **400**, 032042 (2012).
- [12] M. Matsumoto, B. Normand, T. M. Rice, and M. Sigrist, Field- and pressure-induced magnetic quantum phase transitions in TiCuCl_3 , *Phys. Rev. B* **69**, 054423 (2004).
- [13] M. Matsumoto, H. Kuroe, A. Oosawa, and T. Sekine, One-magnon Raman scattering as a probe of longitudinal excitation mode in spin dimer systems, *J. Phys. Soc. Jpn.* **77**, 033702 (2008).
- [14] J. Goldstone, A. Salam, and S. Weinberg, Broken symmetries, *Phys. Rev.* **127**, 965 (1962).
- [15] P. W. Higgs, Broken Symmetries and the Masses of Gauge Bosons, *Phys. Rev. Lett.* **13**, 508 (1964).
- [16] S. Sachdev, *Quantum Phase Transitions*, 2nd ed. (Cambridge University, Cambridge, England, 2011).
- [17] D. Podolsky, A. Auerbach, and D. P. Arovas, Visibility of the amplitude (Higgs) mode in condensed matter, *Phys. Rev. B* **84**, 174522 (2011).
- [18] M. Matsumoto, H. Kuroe, T. Sekine, and T. Masuda, Transverse and longitudinal excitation modes in interacting multispin systems, *J. Phys. Soc. Jpn.* **79**, 084703 (2010).
- [19] M. Hase, M. Kohno, H. Kitazawa, O. Suzuki, K. Ozawa, G. Kido, M. Imai, and X. Hu, Coexistence of a nearly spin-singlet state and antiferromagnetic long-range order in quantum spin system $\text{Cu}_2\text{CdB}_2\text{O}_6$, *Phys. Rev. B* **72**, 172412 (2005).
- [20] M. Hase, A. Dönni, V. Yu. Pomjakushin, L. Keller, F. Gozzo, A. Cervellino, and M. Kohno, Magnetic structure of $\text{Cu}_2\text{CdB}_2\text{O}_6$ exhibiting a quantum-mechanical magnetization plateau and classical antiferromagnetic long-range order, *Phys. Rev. B* **80**, 104405 (2009).
- [21] M. Hase, K. Nakajima, S. Ohira-Kawamura, Y. Kawakita, T. Kikuchi, and M. Matsumoto, Magnetic excitations in the spin- $\frac{1}{2}$ tetramer substance $\text{Cu}_2^{114}\text{Cd}^{11}\text{B}_2\text{O}_6$ obtained by inelastic neutron scattering experiments, *Phys. Rev. B* **92**, 184412 (2015).
- [22] T. Masuda, A. Zheludev, B. Grenier, S. Imai, K. Uchinokura, E. Ressouche, and S. Park, Cooperative Ordering of Gapped and Gapless Spin Networks in $\text{Cu}_2\text{Fe}_2\text{Ge}_4\text{O}_{13}$, *Phys. Rev. Lett.* **93**, 077202 (2004).
- [23] T. Masuda, A. Zheludev, B. Sales, S. Imai, K. Uchinokura, and S. Park, Magnetic excitations in the weakly coupled spin dimers and chains material $\text{Cu}_2\text{Fe}_2\text{Ge}_4\text{O}_{13}$, *Phys. Rev. B* **72**, 094434 (2005).
- [24] T. Masuda, K. Kakurai, M. Matsuda, K. Kaneko, and N. Metoki, Indirect magnetic interaction mediated by a spin dimer in $\text{Cu}_2\text{Fe}_2\text{Ge}_4\text{O}_{13}$, *Phys. Rev. B* **75**, 220401(R) (2007).
- [25] T. Masuda, K. Kakurai, and A. Zheludev, Spin dimers in the quantum ferrimagnet $\text{Cu}_2\text{Fe}_2\text{Ge}_4\text{O}_{13}$ under staggered and random magnetic fields, *Phys. Rev. B* **80**, 180412(R) (2009).
- [26] M. Hase, K. M. S. Etheredge, S.-J. Hwu, K. Hirota, and G. Shirane, Spin-singlet ground state with energy gaps in Cu_2PO_4 : Neutron-scattering, magnetic-susceptibility, and ESR measurements, *Phys. Rev. B* **56**, 3231 (1997); in this reference, the Hamiltonian is defined as $\mathcal{H} = \sum_{i,j} 2J_{ij} S_i \cdot S_j$ instead of $\mathcal{H} = \sum_{i,j} J_{ij} S_i \cdot S_j$ in the present paper.
- [27] I. Živković, D. M. Djokić, M. Herak, D. Pajić, K. Prša, P. Pattison, D. Dominko, Z. Micković, D. Cinčić, L. Forró, H. Berger, and H. M. Rønnow, Site-selective quantum correlations revealed by magnetic anisotropy in the tetramer system SeCuO_3 , *Phys. Rev. B* **86**, 054405 (2012).
- [28] P. Moser, V. Cirpus, and W. Jung, CuInOVO_4 —Single Crystals of a Copper(II) Indium Oxide Vanadate by Oxidation of Cu/In/V Alloys, *Z. Anorg. Allg. Chem.* **625**, 714 (1999).
- [29] J. Rodríguez-Carvajal, Recent advances in magnetic structure determination by neutron powder diffraction, *Physica B* **192**, 55 (1993); <http://www.ill.eu/sites/fullprof/>.
- [30] The estimation of the magnetic specific heat strongly depends on the estimation of the lattice specific heat. There is no non-magnetic isostructural compound for CuInVO_5 . The magnetic specific heat probably remains up to a high T because of the low-dimensional spin system. We cannot determine whether the magnetic specific heat estimated on the basis of an assumption of the lattice specific heat is correct or not. Accordingly, we did not estimate the magnetic specific heat.
- [31] J. C. Bonner and M. F. Fisher, Linear magnetic chains with anisotropic coupling, *Phys. Rev.* **135**, A640 (1964).
- [32] M. Hase, I. Terasaki, and K. Uchinokura, Observation of the Spin-Peierls Transition in Linear Cu^{2+} (Spin- $\frac{1}{2}$) Chains in an Inorganic Compound CuGeO_3 , *Phys. Rev. Lett.* **70**, 3651 (1993).
- [33] M. Hase, I. Terasaki, Y. Sasago, K. Uchinokura, and H. Obara, Effects of Substitution of Zn for Cu in the Spin-Peierls Cuprate, CuGeO_3 : The Suppression of the Spin-Peierls Transition and the Occurrence of a New Spin-Glass State, *Phys. Rev. Lett.* **71**, 4059 (1993).
- [34] M. Hase, I. Terasaki, K. Uchinokura, M. Tokunaga, N. Miura, and H. Obara, Magnetic phase diagram of the spin-Peierls cuprate CuGeO_3 , *Phys. Rev. B* **48**, 9616 (1993).

- [35] M. Hase, M. Kohno, H. Kitazawa, N. Tsujii, O. Suzuki, K. Ozawa, G. Kido, M. Imai, and X. Hu, $1/3$ magnetization plateau observed in the spin- $1/2$ trimer chain compound $\text{Cu}_3(\text{P}_2\text{O}_6\text{OH})_2$, *Phys. Rev. B* **73**, 104419 (2006).
- [36] M. Hase, M. Matsuda, K. Kakurai, K. Ozawa, H. Kitazawa, N. Tsujii, A. Dönni, M. Kohno, and X. Hu, Direct observation of the energy gap generating the $1/3$ magnetization plateau in the spin- $1/2$ trimer chain compound $\text{Cu}_3(\text{P}_2\text{O}_6\text{OD})_2$ by inelastic neutron scattering measurements, *Phys. Rev. B* **76**, 064431 (2007).